

Oxalate-Bridged Bimetallic Complexes $\{\text{NH}(\text{pro})_3\}[\text{M}^{\text{II}}\text{Cr}^{\text{III}}(\text{ox})_3]$ ($\text{M} = \text{Mn}^{\text{II}}, \text{Fe}^{\text{II}}, \text{Co}^{\text{II}}$; $\text{NH}(\text{pro})_3^+ =$ Tri(3-hydroxypropyl)ammonium) Exhibiting Coexistent Ferromagnetism and Proton Conduction

Hisashi Ōkawa,^{*,†,§} Akihito Shigematsu,[†] Masaaki Sadakiyo,^{†,||} Takuya Miyagawa,[‡]
Ko Yoneda,[‡] Masaaki Ohba,^{‡,§} and Hiroshi Kitagawa^{*,†,§,||}

Department of Chemistry, Faculty of Science, Kyushu University, Hakozaki 8-10-1, Higashi-ku,
Fukuoka 812-8581, Japan, Department of Synthetic Chemistry and Biological Chemistry,
Graduate School of Engineering, Kyoto University, Katsura, Nishikyo-ku, Kyoto 615-8510,
Japan, and JST-CREST, Sanban-cho 5, Chiyoda-ku, Tokyo 102-0075, Japan

Received June 30, 2009; E-mail: ok134@chem.kyushu-univ.jp; kitagawa@kuchem.kyoto-u.ac.jp

Abstract: The oxalate-bridged bimetallic complexes $\{\text{NH}(\text{pro})_3\}[\text{M}^{\text{II}}\text{Cr}^{\text{III}}(\text{ox})_3]$ ($\text{M}^{\text{II}} = \text{Mn}^{\text{II}}, \text{Fe}^{\text{II}}, \text{Co}^{\text{II}}$) with hydrophilic tri(3-hydroxypropyl)ammonium ($\text{NH}(\text{pro})_3^+$) were prepared by a new synthetic procedure, and the effects of the $\text{NH}(\text{pro})_3^+$ ion upon the structure, magnetism, and electrical conduction were studied. An X-ray crystallographic study of the MnCr dihydrate, $\{\text{NH}(\text{pro})_3\}[\text{MnCr}(\text{ox})_3] \cdot 2\text{H}_2\text{O}$, was performed. Crystal data: hexagonal, $P6_3$, $a = b = 9.3808(14) \text{ \AA}$, $c = 15.8006(14) \text{ \AA}$, $Z = 2$. The structure comprises oxalate-bridged bimetallic layers interleaved by $\text{NH}(\text{pro})_3^+$ ions. The ions assume a tripodal configuration and are hydrogen bonded to the bimetallic layers together with water molecules, giving rise to a short interlayer separation (7.90 Å) and unsymmetrical faces to the bimetallic layer. Cryomagnetic studies demonstrate ferromagnetic ordering with transition temperature of 5.5 K for the MnCr complex, 9.0 K for the FeCr complex, and 10.0 K for the CoCr complex. The interlayer magnetic interaction is negligibly weak in all of the complexes despite the short interlayer separation. A slow magnetization is observed in all the complexes. This is explained by spin canting associated with the unsymmetrical feature of the bimetallic layer. The complexes show proton conduction of 1.2×10^{-10} to $4.4 \times 10^{-10} \text{ S cm}^{-1}$ under 40% relative humidity (RH) and $\sim 1 \times 10^{-4} \text{ S cm}^{-1}$ under 75% RH. On the basis of water adsorption/desorption profiles, the conduction under 40% RH is mediated through the hydrogen-bonded network formed by the bimetallic layer, $\text{NH}(\text{pro})_3^+$ ions, and water molecules (two per MCr). Under 75% RH, additional water molecules (three per MCr) are concerned with the high proton conduction. This is the first example of a metal complex system exhibiting coexistent ferromagnetism and proton conduction.

Introduction

Since ferromagnetic ordering in $\{\text{N}(n\text{-C}_4\text{H}_9)_4\}[\text{M}^{\text{II}}\text{Cr}^{\text{III}}(\text{ox})_3]$ was first recognized,¹ oxalate-bridged bimetallic complexes of the $(\text{A})[\text{M}^{\text{II}}\text{M}^{\text{III}}(\text{ox})_3]$ type have been extensively studied as novel molecular magnets.^{2–9} In this family of magnetic compounds, tri(oxalato)metalate(III), $[\text{M}^{\text{III}}(\text{ox})_3]^-$, bridges three

M^{II} ions through its oxalate groups, constructing a two-dimensional honeycomb network in which each M^{II} ion is surrounded by three M^{III} ions and vice versa. Ferro-, ferri-, or canted antiferromagnets with critical temperatures ranging from 5 to 44 K have been obtained by the combination of M^{II} and M^{III} ions. A bulky cation (A^+) is necessary to stabilize the network structure of $(\text{A})[\text{M}^{\text{II}}\text{M}^{\text{III}}(\text{ox})_3]$, where the cations are

[†] Kyushu University.

[‡] Kyoto University.

[§] JST-CREST.

^{||} Present address: Department of Chemistry, Graduate School of Science, Kyoto University, Kitashirakawa-Oiwakecho, Sakyo-ku, Kyoto 606-8502, Japan.

(1) (a) Zhong, Z. J.; Matsumoto, N.; Ōkawa, H.; Kida, S. *Chem. Lett.* **1990**, 87. (b) Tamaki, H.; Zhong, Z. J.; Matsumoto, N.; Kida, S.; Koikawa, M.; Achiwa, N.; Hashimoto, Y.; Ōkawa, H. *J. Am. Chem. Soc.* **1992**, *114*, 6974.

(2) (a) Tamaki, H.; Mitsumi, M.; Nakamura, N.; Matsumoto, N.; Kida, S.; Ōkawa, H.; Iijima, S. *Chem. Lett.* **1992**, 1975. (b) Ōkawa, H.; Matsumoto, N.; Tamaki, H.; Ohba, N. *Mol. Cryst. Liq. Cryst.* **1993**, *232*, 617.

(3) (a) Decurtins, S.; Schmalte, H. W.; Oswald, H. R.; Linden, A.; Ensling, J.; Gütlich, P.; Hauser, A. *Inorg. Chim. Acta* **1994**, *216*, 65. (b) Pellaux, R.; Schmalte, H. W.; Huber, R.; Fisher, P.; Hauss, T.; Ouladiff, B.; Decurtins, S. *Inorg. Chem.* **1997**, *36*, 2301.

(4) (a) Mathonière, C.; Carling, S. G.; Yusheng, D.; Day, P. *J. Chem. Soc., Chem. Commun.* **1994**, 1551. (b) Mathonière, C.; Nuttall, C. J.; Carling, S. G.; Day, P. *Inorg. Chem.* **1996**, *35*, 1201.

(5) Carling, S. G.; Mathonière, C.; Day, P.; Malik, K. M. A.; Coles, S. J.; Hursthouse, M. B. *J. Chem. Soc., Dalton Trans.* **1996**, 1839.

(6) Min, K. S.; Miller, J. S. *J. Chem. Soc., Dalton Trans.* **2006**, 2463.

(7) Shilov, G. V.; Atovmjan, L. O.; Ovanesyan, N. S.; Pyalling, A. A.; Bottyan, L. *Russ. J. Coord. Chem.* **1998**, *24*, 288.

(8) (a) Coronado, E.; Galán-Mascarós, J. R.; Gómez-García, C. J.; Martínez-Agudo, J. M.; Martínez-Ferrero, E.; Waerenborgh, J. C.; Almeida, M. *J. Solid State Chem.* **2001**, *159*, 391. (b) Coronado, E.; Galán-Mascarós, J. R.; Martí-Gastaldo, C. *J. Mater. Chem.* **2006**, *16*, 2685.

(9) (a) Clemente-León, M.; Coronado, E.; Galán-Mascarós, J. R.; Gómez-García, C. *J. Chem. Soc., Chem. Commun.* **1997**, 1727. (b) Coronado, E.; Galán-Mascarós, J. R.; Gómez-García, C. J.; Martínez-Agudo, J. M. *Adv. Mater.* **1999**, *11*, 558.

intercalated between the bimetallic layers. Taking advantage of the layered structure of the oxalate-bridged bimetallic complexes, attention has recently been paid to the development of multifunctional magnetic materials by the use of a magnetic cation,¹⁰ a photoactive cation,¹¹ a conductive cation,¹² or a chiral cation¹³ instead of “innocent” cations.

Recently, much attention had been paid to network compounds made of complex constituents with the aim of producing functional materials such as conducting materials, magnetic materials, and so on.^{14–21} The development of new proton-conductive materials is becoming particularly important in relation to energy technology.^{22,23} We have previously reported on *N,N'*-bis(2-hydroxyethyl)dithiooxamidatocopper(II) and *N,N'*-bis(3-hydroxypropyl)dithiooxamidatocopper(II), with a layered structure of binuclear copper units, as proton-conductive systems.²³ In these complexes, the 2-hydroxyethyl or 3-hydroxypropyl groups aligned in a 2-D manner are responsible for the proton conduction.

We are interested in developing new proton-conductive systems based on the layered structure of the oxalate-bridged bimetallic complexes. Our strategy for this purpose is to

introduce hydroxyl (OH) groups into the alkyl residue of ammonium ions so as to provide hydrophilic layers of OH groups as conductive pathways of proton in the 2-D network structure. In this study, the tri(3-hydroxypropyl)ammonium ion, $\{\text{NH}(\text{pro})_3\}^+$, is used as such a hydrophilic cation to obtain the following bimetallic complexes: $\{\text{NH}(\text{pro})_3\}[\text{M}(\text{ox})_3]$ ($\text{M} = \text{Mn}^{\text{II}}, \text{Fe}^{\text{II}}, \text{Co}^{\text{II}}$). The effects of the cation upon the structure, magnetism and electrical conduction of the bimetallic complexes are studied.

Experimental Section

Materials. All chemicals were of reagent grade and were used as commercially purchased. A standard literature procedure²⁴ was used for the preparation of $(\text{NH}_4)_3[\text{Cr}(\text{ox})_3] \cdot 3\text{H}_2\text{O}$. Tri(3-hydroxypropyl)amine was prepared by a method described in the literature²⁵ and then converted into tri(3-hydroxypropyl)ammonium chloride, $\{\text{NH}(\text{pro})_3\}\text{Cl}$, by treatment with hydrochloric acid.

Preparation of Bimetallic Complexes. $\{\text{NH}(\text{pro})_3\}[\text{MnCr}(\text{ox})_3] \cdot \text{H}_2\text{O}$. To a methanol solution (30 cm³) of $(\text{NH}_4)_3[\text{Cr}(\text{ox})_3] \cdot 3\text{H}_2\text{O}$ (428 mg, 1×10^{-3} mol) and $\text{MnCl}_2 \cdot 4\text{H}_2\text{O}$ (198 mg, 1×10^{-3} mol) was added a methanol solution (5 cm³) of $\{\text{NH}(\text{pro})_3\}\text{Cl}$ (228 mg, 1×10^{-3} mol). Resulting purple microcrystals were separated by filtration, washed with methanol, and dried over silica gel under vacuum. The yield was 430 mg (74%). Elemental analysis (%) calcd for $\text{C}_{15}\text{H}_{24}\text{NO}_{16}$ CrMn: C, 30.99; H, 4.16; N, 2.41; Cr, 8.94; Mn, 9.45. Found: C, 31.26; H, 4.29; N, 2.38; Cr, 8.69; Mn, 9.71. Visible bands on powder (λ , nm): 570, 420, 280. FT-IR (cm⁻¹): 1647.

$\{\text{NH}(\text{pro})_3\}[\text{Fe}(\text{Cr}(\text{ox})_3)] \cdot \text{H}_2\text{O}$. This was obtained as reddish-brown microcrystals in a similar way as the MnCr complex except that general precautions to avoid oxidation by atmospheric oxygen were taken. The yield was 340 mg (58%). Elemental analysis (%) calcd for $\text{C}_{15}\text{H}_{24}\text{NO}_{16}$ CrFe: C, 30.94; H, 4.15; N, 2.41; Cr, 8.93; Fe, 9.59. Found: C, 31.37; H, 4.27; N, 2.43; Cr, 9.26; Fe, 9.25. Visible bands on powder (λ , nm): 575, 415, 280. FT-IR (cm⁻¹): 1630.

$\{\text{NH}(\text{pro})_3\}[\text{CoCr}(\text{ox})_3] \cdot \text{H}_2\text{O}$. This was obtained as pink microcrystals in the same way as the MnCr complex. The yield was 390 mg (67%). Elemental analysis (%) calcd for $\text{C}_{15}\text{H}_{24}\text{NO}_{16}$ CoCr: C, 30.78; H, 4.13; N, 2.39; Co, 10.07; Cr, 8.88. Found: C, 30.58; H, 4.12; N, 2.43; Co, 9.70; Cr, 9.25. Visible bands on powder (λ , nm): 555, 420, 290. FT-IR (cm⁻¹): 1626.

Physical Measurements. Elemental analyses of C, H, and N were carried out at the Elemental Analysis Service Center of Kyushu University. Metal analyses were obtained with a Rigaku wavelength dispersive X-ray fluorescence ZSX 100s. Magnetic measurements were performed using a Quantum Design MPMS-XL5R SQUID susceptometer. Molar magnetic susceptibilities (χ_{M}) were corrected for the diamagnetism of constituting atoms using Pascal's constants.²⁶ Weak-field magnetization studies (field-cooled magnetization, zero-field-cooled magnetization, remnant magnetization) were carried out under an applied field of 20 gauss. Field-dependence of magnetization was measured in the applied field up to 50 kOe at 2 K. For AC conductivity measurements, sample pellets of ~0.8 mm thickness and 2.5 mm ϕ were prepared under a pressure of ~1.2 GPa. The impedance measurements were carried out by the conventional quasi-four-probe method using gold paste and gold wires (50 μm ϕ) with a Solartron SI 1260 Impedance/Gain-Phase Analyzer and 1296 Dielectric Interface in the frequency range 1 Hz–1 MHz, at 298 K. Relative humidity (RH) was controlled by using an Espec Corp. SH-221 incubator. The measurement of water adsorption isotherms was carried out at 298 K with an automatic vapor adsorption apparatus, BELSORP-max (BEL JAPAN). Samples were thoroughly dehydrated prior to the measurement by heating

- (10) Coronado, E.; Galán-Mascarós, J. R.; Gómez-García, C. J.; Ensling, J.; Gütllich, P. *Chem.–Eur. J.* **2000**, *6*, 552.
- (11) (a) Bénard, S.; Rivière, E.; Yu, P.; Nakatani, K.; Delouis, J. F. *Chem. Mater.* **2001**, *13*, 159. (b) Bénard, S.; Yu, P.; Audière, J. P.; Rivière, E.; Clément, R.; Guilhem, J.; Tchertanov, L.; Nakatani, K. *J. Am. Chem. Soc.* **2000**, *122*, 9444.
- (12) (a) Coronado, E.; Galán-Mascarós, J. R.; Gómez-García, C. J.; Laukhin, V. *Nature* **2000**, *408*, 447. (b) Alberola, A.; Coronado, E.; Galán-Mascarós, J. R.; Giménez-Saiz, C.; Gómez-García, C. J.; Romero, F. M. *Synth. Met.* **2003**, *133–134*, 509. (c) Alberola, A.; Coronado, E.; Galán-Mascarós, J. R.; Giménez-Saiz, C.; Gómez-García, C. J.; Martínez-Ferrero, E.; Murcia-Martínez, A. *Synth. Met.* **2003**, *135–136*, 687. (d) Alberola, A.; Coronado, E.; Galán-Mascarós, J. R.; Giménez-Saiz, C.; Gómez-García, C. J. *J. Am. Chem. Soc.* **2003**, *125*, 10774.
- (13) Train, C.; Gheorghie, R.; Krstic, V.; Chamoreau, L. M.; Ovanesyan, N. S.; Rikken, G. L. J. A.; Gruselle, M.; Verdager, M. *Nat. Mater.* **2008**, *7*, 729.
- (14) Sessoli, R.; Gatteschi, D.; Caneschi, A.; Navak, M. A. *Nature* **1993**, *365*, 141.
- (15) Kitagawa, H.; Onodera, N.; Sonoyama, T.; Yamamoto, M.; Fukawa, T.; Mitani, T.; Seto, M.; Maeda, Y. *J. Am. Chem. Soc.* **1999**, *121*, 10068.
- (16) (a) Kurmoo, M.; Graham, A. W.; Day, P.; Coles, S. J.; Hursthouse, M. B.; Caulfield, J. L.; Singleton, J.; Pratt, F. L.; Hays, W. *J. Am. Chem. Soc.* **1995**, *117*, 12209. (b) Akutsu, H.; Akutsu-Sato, A.; Turner, S. S.; Pevelen, D. L.; Day, P.; Laukhin, V.; Klehe, A.; Singleton, J.; Tocher, D. A.; Probert, M. R.; Howard, J. A. K. *J. Am. Chem. Soc.* **2002**, *124*, 12430. (c) Akutsu-Sato, A.; Akutsu, H.; Turner, S. S.; Day, P.; Probert, M. R.; Howard, J. A. K.; Akutagawa, T.; Takeda, S.; Nakamura, T.; Mori, T. *Angew. Chem.* **2005**, *117*, 296.
- (17) Rosi, N. L.; Eckert, J.; Eddaoudi, M.; Vodak, D. T.; Kim, J.; O'Keeffe, M.; Yagi, O. M. *Science* **2003**, *300*, 1127.
- (18) Kitagawa, S.; Kitaura, R.; Noro, S. *Angew. Chem., Int. Ed.* **2004**, *43*, 2334.
- (19) *Extended Linear Chain Compounds*; Miller, J. S., Ed.; Plenum Press: New York, 1982.
- (20) *Inorganic Materials*; Bruce, D. W., O'Hara, D., Eds.; Wiley: Chichester, 1992.
- (21) Heger, G.; Deiseroth, H. J.; Schultz, H. *Acta Crystallogr.* **1978**, *B34*, 725.
- (22) (a) Sadakiyo, M.; Yamada, T.; Kitagawa, H. *J. Am. Chem. Soc.* **2009**, *131*, 9906. (b) Yamada, T.; Sadakiyo, M.; Kitagawa, H. *J. Am. Chem. Soc.* **2009**, *131*, 3144. (c) Yamada, T.; Kitagawa, H. *J. Am. Chem. Soc.* **2009**, *131*, 6312.
- (23) (a) Fujishima, M.; Kanda, S.; Mitani, T.; Kitagawa, H. *Synth. Met.* **2001**, *119*, 485. (b) Nagao, Y.; Ikeda, R.; Kanda, S.; Kubozono, Y.; Kitagawa, H. *Mol. Cryst. Liq. Cryst.* **2002**, *379*, 89. (c) Nagao, Y.; Fujishima, M.; Kanda, S.; Ikeda, R.; Kitagawa, H. *Synth. Met.* **2003**, *133–134*, 431. (d) Nagao, Y.; Ikeda, R.; Iijima, K.; Kubo, T.; Nakasuji, K.; Kitagawa, H. *Synth. Met.* **2003**, *135–136*, 283. (e) Nagao, Y.; Kubo, T.; Nakasuji, K.; Ikeda, R.; Kojima, T.; Kitagawa, H. *Synth. Met.* **2005**, *154*, 89.

(24) Bailar, J. C., Jr.; Jones, E. M. *Inorg. Synth.* **1939**, *1*, 37.

(25) Levason, W.; Sheikh, B. *J. Organomet. Chem.* **1981**, *209*, 161.

(26) *Landolt-Börnstein, Neue Series III/11*; Springer-Verlag: Berlin, 1981.

at 373 K for 16 h under vacuum. Solid-state circular dichroism spectra were measured on a JASCO J-820 circular dichroism spectrometer using KBr pellet with 1% sample content.

Crystal Structure Determination. Purple prismatic crystals of $\{\text{NH}(\text{pro})_3\}[\text{MnCr}(\text{ox})_3] \cdot 2\text{H}_2\text{O}$ were grown by slow crystallization from a dilute methanol solution of $(\text{NH}_4)_3[\text{Cr}(\text{ox})_3] \cdot 3\text{H}_2\text{O}$, $\text{MnCl}_2 \cdot 4\text{H}_2\text{O}$ and $\{\text{NH}(\text{pro})_3\}\text{Cl}$. X-ray diffraction data were collected on a Bruker SMART APEX CCD-detector diffractometer with graphite-monochromated Mo K α radiation ($\lambda = 0.71069 \text{ \AA}$), using a single crystal with approximate dimensions of $0.22 \times 0.22 \times 0.04 \text{ mm}^3$. The structure was solved by a direct method and expanded using Fourier techniques. All calculations were performed using the CrystalStructure crystallographic software package.²⁷ Full-matrix least-squares refinements were carried out using SHELXL-97²⁸ with anisotropic thermal parameters for nonhydrogen atoms.

Crystal data for $\{\text{NH}(\text{pro})_3\}[\text{MnCr}(\text{ox})_3] \cdot 2\text{H}_2\text{O}$ at 100 K: purple crystals, $\text{C}_{15}\text{H}_{26}\text{CrMnNO}_{17}$, molecular weight = 599.30, hexagonal, space group $P6_3$, $Z = 2$, $a = b = 9.3808(14) \text{ \AA}$, $c = 15.8006(14) \text{ \AA}$, $\alpha = \beta = 90^\circ$, $\gamma = 120^\circ$, $V = 1204.2(3) \text{ \AA}^3$, $D_{\text{calcd}} = 1.642 \text{ g cm}^{-3}$, $\mu(\text{Mo K}\alpha) = 10.559 \text{ cm}^{-1}$, $R_1 = 0.0805$ ($I > 2.0\sigma(I)$), $R = 0.0841$ (all reflections), $wR_2 = 0.2283$ (all reflections). Symmetry operations: (1) $-Y, X - Y, Z$; (2) $-X + Y, -X, Z$; (3) $X - 1, Y, Z$; (4) $-Y, X - Y - 1, Z$; (5) $-X + Y + 1, -X + 1, Z$; (6) $-Y + 1, X - Y, Z$.

Results and Discussion

Preparation and General Characterization. The oxalate-bridged bimetallic complexes, $(\text{A})[\text{M}^{\text{II}}\text{M}^{\text{III}}(\text{ox})_3]$, have generally been prepared by the reaction of $\text{K}_3[\text{M}'(\text{ox})_3]$, a M(II) salt, and an A^+ salt in water. Despite repeated efforts, however, our attempts to prepare $\{\text{NH}(\text{pro})_3\}[\text{MCr}(\text{ox})_3]$ complexes by a similar reaction were unsuccessful. It is presumed that the bimetallic network structure with $\text{NH}(\text{pro})_3^+$ ions is unstable in aqueous solution because of the hydrophilicity of the $\text{NH}(\text{pro})_3^+$ ion. The synthesis of $\{\text{NH}(\text{pro})_3\}[\text{MCr}(\text{ox})_3]$ can be achieved in an organic solvent of low dielectric constant, but many difficulties arise during the synthesis because $\text{K}_3[\text{Cr}(\text{ox})_3]$ is insoluble in most organic solvents. Coronado used 18-crown-6 in the synthesis of oxalate-bridged bimetallic complexes using $\text{K}_3[\text{Cr}(\text{ox})_3]$ in methanol, to obtain $\{\text{K}(18\text{-crown-6})\}[\text{M}(\text{H}_2\text{O})_2\text{Cr}(\text{ox})_3]$ ($\text{M} = \text{Mn}^{\text{II}}, \text{Co}^{\text{II}}$).^{29,30} We followed up this synthesis by adding $\{\text{NH}(\text{pro})_3\}\text{Cl}$ to the reaction solution but failed to isolate the desired complexes. In the ongoing search for synthetic methods for oxalate-bridged bimetallic complexes in an organic solvent, it became apparent that ammonium tri(oxalato)chromate(III), $(\text{NH}_4)_3[\text{Cr}(\text{ox})_3]$, is moderately soluble in methanol and becomes more soluble upon addition of a transition M(II) salt. Thus, a new synthetic procedure for $(\text{A})[\text{MCr}(\text{ox})_3]$ complexes that involves the use of $(\text{NH}_4)_3[\text{Cr}(\text{ox})_3]$ in methanol is proposed.

In our first attempt, tetra(3-hydroxypropyl)ammonium chloride, $\{\text{N}(\text{pro})_4\}\text{Cl}$, was used with the intention of obtaining $\{\text{N}(\text{pro})_4\}[\text{MCr}(\text{ox})_3]$, but the analytical data of the resulting products coincided with those of $\{\text{NH}(\text{pro})_3\}[\text{MCr}(\text{ox})_3] \cdot \text{H}_2\text{O}$ ($\text{M} = \text{Mn}^{\text{II}}, \text{Fe}^{\text{II}}, \text{Co}^{\text{II}}$). The formula of the products was confirmed by experiments using $\{\text{NH}(\text{pro})_3\}\text{Cl}$ instead of $\{\text{N}(\text{pro})_4\}\text{Cl}$. It is likely that during the course of complex formation, $\text{N}(\text{pro})_4^+$ is converted into $\text{NH}(\text{pro})_3^+$, with the

elimination of allyl alcohol. Oxalate-bridged $\text{Fe}^{\text{II}}\text{Cr}^{\text{III}}$ complexes are often contaminated by an Fe^{III} species.¹⁰ The synthesis of the FeCr complex was carried out under nitrogen in order to avoid oxidation by atmospheric oxygen.

One bimetallic complex of a tertiary ammonium ion, $\{\text{NH}(n\text{-C}_3\text{H}_7)_3\}[\text{MnCr}(\text{ox})_3]$, has been reported.³¹ This was inadvertently obtained by a gel-technique reaction of $(\text{NH}_4)_3[\text{Cr}(\text{ox})_3]$, $\text{Mn}(\text{NO}_3)_2 \cdot 6\text{H}_2\text{O}$ and a ferrocene derivative with a $-\text{CH}_2\text{N}^+(n\text{-C}_3\text{H}_7)_3$ group in one cyclopentadienyl ligand. It is noted that $\{\text{NH}(n\text{-C}_3\text{H}_7)_3\}[\text{MnCr}(\text{ox})_3]$ is hardly precipitated during the usual synthesis in an aqueous solution. We have confirmed that the present synthetic procedure is applicable to a fairly wide range of $(\text{A})[\text{MCr}(\text{ox})_3]$ complexes, including those of less bulky ammonium ions such as $\{\text{N}(\text{C}_2\text{H}_5)_4\}[\text{MnCr}(\text{ox})_3]$ as well as $\{\text{NH}(n\text{-C}_3\text{H}_7)_3\}[\text{MnCr}(\text{ox})_3]$.

All of the complexes are sensitive to moisture and decompose instantly in water. The IR spectra of the complexes show a distinct $\nu_{\text{as}}(\text{C}=\text{O})$ vibration of the oxalate group at $1647\text{--}1626 \text{ cm}^{-1}$, in marked contrast to $(\text{NH}_4)_3[\text{Cr}(\text{ox})_3]$, which exhibits two $\nu_{\text{as}}(\text{C}=\text{O})$ bands at 1716 and 1686 cm^{-1} and one $\nu_{\text{s}}(\text{C}=\text{O})$ band at 1400 cm^{-1} . The IR spectral feature with one $\nu_{\text{as}}(\text{C}=\text{O})$ at lower frequency is consistent with the oxalate-bridged network structure of the MCr complexes. In the reflectance spectra, three absorption bands are seen at $555\text{--}575$, $415\text{--}420$, and $280\text{--}290 \text{ nm}$, which are assigned to the ${}^4\text{T}_{2g} \leftarrow {}^4\text{A}_{2g}$, ${}^4\text{T}_{1g}(\text{F}) \leftarrow {}^4\text{A}_{2g}$ and ${}^4\text{T}_{1g}(\text{P}) \leftarrow {}^4\text{A}_{2g}$ transitions, respectively, of the $\{\text{Cr}^{\text{III}}(\text{ox})_3\}$ chromophore in O_h symmetry approximation. The d-d bands of the $\{\text{M}^{\text{II}}(\text{ox})_3\}$ ($\text{M} = \text{Mn}, \text{Fe}, \text{Co}$) moiety are not well resolved. The d-d bands of the complexes, except for the first band of the CoCr complex, are shifted to longer wavelengths relative to those of $(\text{NH}_4)_3[\text{Cr}(\text{ox})_3]$ (560 , 395 , and 265 nm), implying a lowering of the $\{\text{Cr}^{\text{III}}(\text{ox})_3\}$ ligand field in the bimetallic network. The first d-d band of the CoCr complex is seen at a shorter wavelength (555 nm) than the corresponding band of $(\text{NH}_4)_3[\text{Cr}(\text{ox})_3]$ (560 nm), probably owing to the superposition of the d-d bands of the $\{\text{Co}^{\text{II}}(\text{ox})_3\}$ chromophore.

Crystal Structure. A crystallographic study of the MnCr dihydrate, $\{\text{NH}(\text{pro})_3\}[\text{MnCr}(\text{ox})_3] \cdot 2\text{H}_2\text{O}$, was carried out. The best solution was obtained in the chiral space group $P6_3$; structural analyses applying any achiral space groups did not converge to normal solution. The Flack parameter of 0.44 in the structural analysis suggests that the crystal can be twin. In accord with this presumption, the MnCr complex is shown to be nonchiral on the basis of solid-state circular dichroism spectra. The crystallographic results reveal characteristics of its network structure despite some uncertainty in the propane chain conformation of the $\text{NH}(\text{pro})_3^+$ ion. The crystal consists of the oxalate-bridged bimetallic layers interleaved by $\text{NH}(\text{pro})_3^+$ ions (Figure 1). The structural features are comparable to those observed for analogous $(\text{A})[\text{MM}'(\text{ox})_3]$ complexes.^{3,5,10,11}

Figure 2a shows a projection of one bimetallic layer and $\{\text{NH}(\text{pro})_3\}^+$ cations onto the crystallographic ab plane. An ORTEP drawing of the $\{(\text{ox})_2\text{Mn}(\text{ox})\text{Cr}(\text{ox})_2\}$ coordination with the labeling scheme is shown in Figure 2b. Selected bond distances and bond angles are summarized in Table 1. The two metal ions are clearly distinguished by the short Cr–O bonds (av 1.993 \AA) and the long Mn–O bonds (av 2.144 \AA). Each $\text{NH}(\text{pro})_3^+$ ion is situated above a Cr and interacts with the bimetallic layer through hydrogen bonding to one donor oxygen $\text{O}(2)$ ($\text{O}(2)^1$ and $\text{O}(2)^2$) of the adjacent $\{\text{Mn}(\text{ox})_3\}$ units in an

(27) CrystalStructure 3.8.0: Crystal Structure Analysis Package; Rigaku and Rigaku/MSK: Tokyo and Woodlands, TX, 2000–2006.

(28) Sheldrick, G. M. SHELXL97; University of Göttingen: Göttingen, Germany, 1997.

(29) Coronado, E.; Galán-Mascarós, J. R.; Gómez-García, C. J.; Martí-Gastaldo, C. *Inorg. Chem.* **2005**, *44*, 6197.

(30) Coronado, E.; Galán-Mascarós, J. R.; Martí-Gastaldo, C. *Inorg. Chem.* **2007**, *46*, 8108.

(31) Shilov, G. V.; Ovanesyan, N. S.; Aldoshin, S. M.; Gruselle, M.; Train, C.; Guyard-Duhayon, C. *J. Coord. Chem.* **2004**, *57*, 1165.

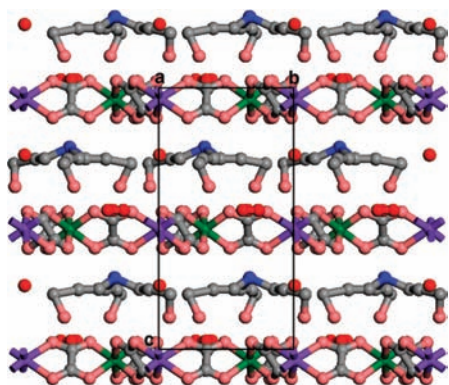


Figure 1. Projection of $\{\text{NH}(\text{pro})_3\}[\text{MnCr}(\text{ox})_3]\cdot 2\text{H}_2\text{O}$ along the crystallographic a axis (green = Cr, purple = Mn; red = water oxygen).

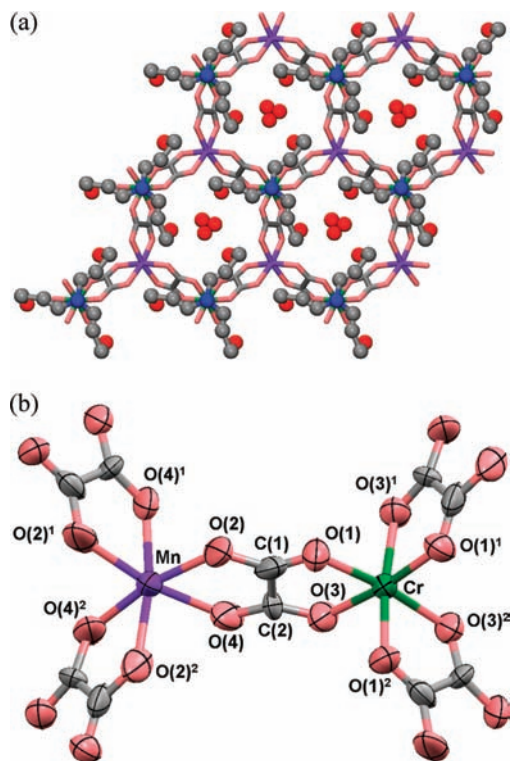


Figure 2. (a) Projection of one bimetallic layer and cations onto the ab plane. The bimetallic network is represented by capped sticks and the cations by balls and sticks. (b) An ORTEP drawing with the labeling scheme of the $\{(\text{ox})_2\text{Mn}(\text{ox})\text{Cr}(\text{ox})_2\}$ coordination (50% probability level).

O–O separation of 3.17 Å. The $\text{NH}(\text{pro})_3^+$ ion assumes a tripodal configuration, with a 3-fold axis along the N–H bond. One water molecule exists in each honeycomb cavity, deviating by 1.14 Å from the Cr_3Mn_3 least-squares plane, and is statistically hydrogen bonded to three hydroxyl oxygen atoms of separate $\text{NH}(\text{pro})_3^+$ ions, with an O–O distance of 2.78 Å. On the opposite side of the bimetallic layer, another water molecule exists, which is hydrogen bonded to one $\{\text{Mn}(\text{ox})_3\}$ in an $\text{O}(\text{water})\text{--O}(4)$ ($\text{O}(4)^1$ and $\text{O}(4)^2$) distance of 2.93 Å. This water is absent in the crystal of the MnCr monohydrate, $\{\text{NH}(\text{pro})_3\}[\text{MnCr}(\text{ox})_3]\cdot \text{H}_2\text{O}$.³² As the result of the hydrogen bonding with $\text{NH}(\text{pro})_3^+$ ions, the bimetallic layer is unsymmetrical with respect to two faces. In fact, both the $\{\text{Mn}(\text{ox})_3\}$

Table 1. Selected Bond Distances and Angles of $\{\text{NH}(\text{pro})_3\}[\text{MnCr}(\text{ox})_3]\cdot 2\text{H}_2\text{O}$

Bond Distances (Å)			
Cr–O(1) ($\text{O}(1)^1$, $\text{O}(1)^2$)	1.969(6)	Cr–O(3) ($\text{O}(3)^1$, $\text{O}(3)^2$)	2.017(6)
Mn–O(2) ($\text{O}(2)^1$, $\text{O}(2)^2$)	2.117(14)	Mn–O(4) ($\text{O}(4)^1$, $\text{O}(4)^2$)	2.171(12)
C(1)–C(2)	1.499(19)	C(1)–O(1)	1.217(17)
C(1)–O(2)	1.311(14)	C(2)–O(3)	1.247(16)
C(2)–O(4)	1.239(17)		
Bond Angles (deg)			
O(1)–Cr–O(1) ¹ ($\text{O}(1)^2$)	93.4(3)	O(2)–Mn–O(2) ¹ ($\text{O}(2)^2$)	98.0(6)
O(1)–Cr–O(3)	82.1(3)	O(2)–Mn–O(4)	76.5(4)
O(1)–Cr–O(3) ¹	92.3(3)	O(2)–Mn–O(4) ¹	91.6(4)
O(1)–Cr–O(3) ²	172.9(3)	O(2)–Mn–O(4) ²	169.5(4)
O(3)–Cr–O(1) ¹	172.9(3)	O(4)–Mn–O(2) ¹	169.5(3)
O(3)–Cr–O(1) ²	92.2(3)	O(4)–Mn–O(2) ²	91.6(4)
O(3)–Cr–O(3) ¹ ($\text{O}(3)^2$)	92.6(2)	O(4)–Mn–O(4) ¹ ($\text{O}(4)^2$)	94.6(5)

and the $\{\text{Cr}(\text{ox})_3\}$ geometries are distorted to C_3 with short metal–oxygen bonds (Cr–O 1.969(6) Å and Mn–O 2.117(14) Å) at the front face to the interacting $\text{NH}(\text{pro})_3^+$ ions and long metal–oxygen bonds (Cr–O 2.017(6) Å and Mn–O 2.171(12) Å) at the other face. This is generally the case in oxalate-bridged bimetallic complexes, but the unsymmetrical feature in the bimetallic layer is most prominent in the present complex because of the cation-layer hydrogen bonding interaction.

The interlayer separations of $(\text{A})[\text{MM}'(\text{ox})_3]$ complexes studied to date vary from 9.96 to 7.93 Å with the bulkiness of the cation^{3,9a,10,11b,32} (a very large interlayer separation has been recognized in the organic π -cation complexes (BEDT-TTF)₃[MnCr(ox)₃] (BEDT-TTF = bis(ethylenedithio)tetrathiafulvalene; interlayer separation 16.61 Å) and (BEDT-TSF)₃[MnCr(ox)₃] (BEDT-TSF = bis(ethylenedithio)tetraselenafulvalene; 20.09 Å)).¹² The present MnCr complex has the shortest interlayer separation (7.90 Å) among the complexes characterized thus far, owing to the folded, tripodal configuration of $\text{NH}(\text{pro})_3^+$ ions.

It is considered that the FeCr and CoCr complexes may have a similar crystal structure judging from the resemblance in powder X-ray diffraction spectra (Figure S1, Supporting Information).

Magnetic Properties. The $X_M T$ value for the MnCr complex at room temperature is 6.04 emu K mol^{−1} (= 6.95 μ_B) per MnCr, which corresponds to the spin-only value for $\text{Mn}^{\text{II}}(\text{S}=5/2)\text{--Cr}^{\text{III}}(\text{S}=3/2)$ (6.25 emu K mol^{−1} (7.07 μ_B)). The $X_M T$ value increases gradually with cooling to 20 K and then sharply to a large value of 106.58 emu K mol^{−1} (29.20 μ_B) at 5 K, indicating the onset of ferromagnetic ordering. Similarly, the $X_M T$ values of the FeCr and the CoCr complexes increase with lowering temperature, from 5.80 emu K mol^{−1} (6.81 μ_B) at room temperature to 209.30 emu K mol^{−1} (40.92 μ_B) at 8 K for the former and from 5.41 emu K mol^{−1} (6.58 μ_B) at room temperature to 282.86 emu K mol^{−1} (47.57 μ_B) at 9.5 K for the latter. To estimate the ferromagnetic transition temperature (T_C), magnetization studies were carried out. The results for the MnCr complex are given in Figure 3. The field-cooled magnetization (FCM) under a weak applied field of 5 Oe shows a sharp increase below 7 K, with an inflection around 5 K, and the dM/dT versus T plots have a minimum peak at 5.5 K (Figure 3, insert). When the applied field is switched off, a remnant magnetization (RM) of 76 emu Oe mol^{−1} at 2 K is observed, which decreases upon warming, until it disappears at ~6 K. The zero-field-cooled magnetization (ZFCM) has a maximum around 5 K. The occurrence of ferromagnetic ordering was also studied by AC magnetic measurements, and the results have enabled us to estimate the

(32) Preliminary crystallographic data ($R_1 = 0.1091$, $R = 0.1120$, and $wR_2 = 0.3462$).

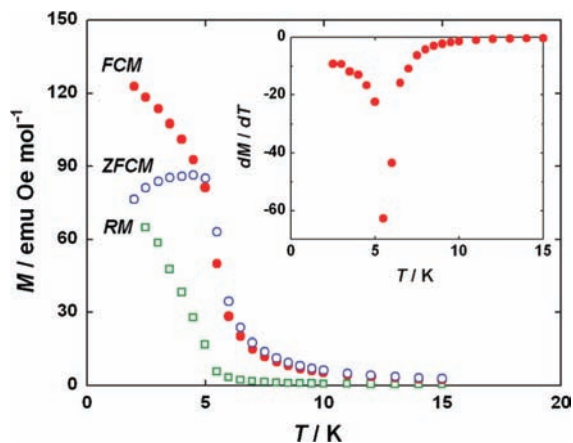


Figure 3. Field-cooled magnetization (FCM) under 5 Oe, remnant magnetization (RM), and zero-field-cooled magnetization (ZFCM) of the MnCr complex. The insert is the dM/dT versus T plot of FCM.

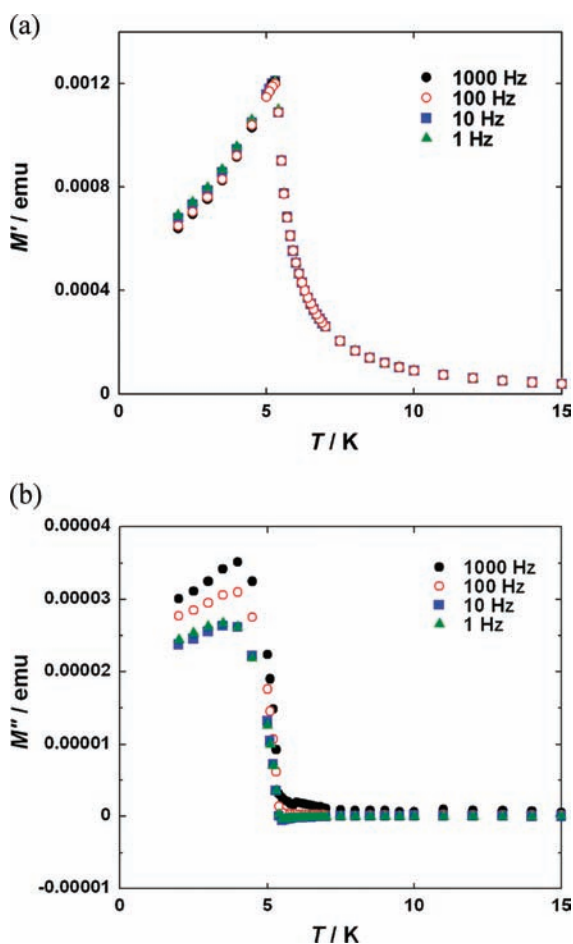


Figure 4. (a) In-phase magnetization (M') and (b) out-of-phase magnetization (M'') curves of the MnCr complex measured in an AC field of 3 Oe at frequencies of 1–1000 Hz.

T_C more precisely (Figure 4). The in-phase magnetization (M') curves measured at frequencies of 1–1000 Hz have a peak at 5.5 K, and the out-of-phase magnetization (M'') curves have nonzero magnetization below 5.5 K. Thus the T_C of the MnCr complex is determined to be 5.5 K. Similarly, the T_C values of the FeCr and CoCr complexes are determined to be 9.0 and 10.0 K, respectively (Figures S2–S5, Supporting Information).

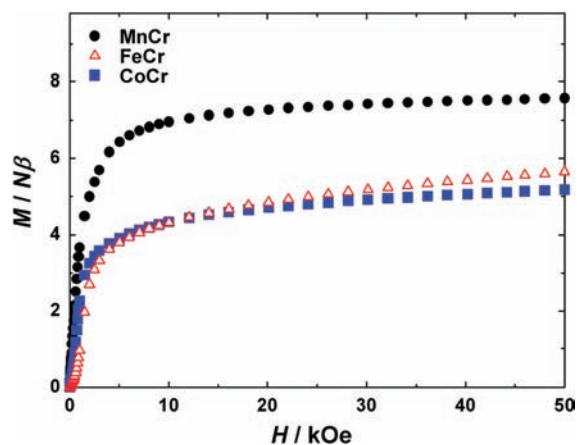


Figure 5. Field-dependence of magnetization of the complexes measured at 2 K.

The T_C values of (A)[MnCr(ox)₃] complexes reported to date fall in the range of 5–6 K, irrespective of the interlayer separation varying from 9.92 to 8.20 Å.^{1,3,10,11b} The T_C values of the organic π -cation complexes (BEDT-TTF)₃[MnCr(ox)₃] and (BEDT-TSF)₃[MnCr(ox)₃] with a large interlayer separation (16.61 and 20.09 Å, respectively) also fall in this range.¹² Therefore, the interlayer magnetic interaction is negligibly weak in the MnCr complex, despite its short interlayer separation. The T_C values of the FeCr and CoCr complexes are also close to those found for analogous (A)[FeCr(ox)₃] and (A)[CoCr(ox)₃] complexes, respectively.^{1,9a,10,11b} In bulk magnetism, (A)[M-Cr(ox)₃] complexes are in marked contrast to the cyanide-bridged layered complexes, [Ni(diamine)₂]₂[Fe(CN)₆]₂X, exhibiting variable magnetism dependent upon the interlayer separation, i.e., ferromagnetism if interlayer separation >10 Å or metamagnetism if separation <10 Å.³³

The field dependence of magnetization measured at 2 K is summarized in Figure 5. The magnetization of the MnCr complex increases rapidly with the magnetic field, relative to the Brillouin function for $S = 8/2$ ($S_{Mn} + S_{Cr}$), but the M versus H curve becomes sluggish around 3 kOe reaching $7.6 N\beta$ at 50 kOe, which is smaller than the expected value of $8 N\beta$. This feature has been noted in analogous (A)[MnCr(ox)₃] complexes and has been explained in terms of the presence of spin canting in the ferromagnetic structure.^{1,3a,10,11b} Slow saturation in magnetization is also seen in the FeCr and the CoCr complexes, where the magnetization approaches $5.65 N\beta$ and $5.17 N\beta$ at 50 kOe, respectively. It is noted that the magnetization values at 50 kOe are much smaller than expected ($7 N\beta$ for FeCr and $6 N\beta$ for CoCr). Because the magnetization behavior of the FeCr complex is particularly anomalous, we reinvestigated the magnetic behavior of this complex using a freshly prepared sample and confirmed the M versus H curve in Figure 5 to be intrinsic of this complex. It appears that the spin canting effect upon magnetization is pronounced in the present complexes because of the distinctly unsymmetrical feature of the bimetallic layer.

The hysteresis curves of the complexes were measured at 2 K (Figure 6). The MnCr complex has a small coercive field of 10 Oe, which is typical of soft magnets. The coercive fields of

(33) (a) Ohba, M.; Ôkawa, H.; Fukita, N.; Hashimoto, Y. *J. Am. Chem. Soc.* **1997**, *119*, 1011. (b) Ohba, M.; Ôkawa, H. *Coord. Chem. Rev.* **2000**, *198*, 313. (c) Ôkawa, H.; Ohba, M. *Bull. Chem. Soc. Jpn.* **2002**, *75*, 1191.

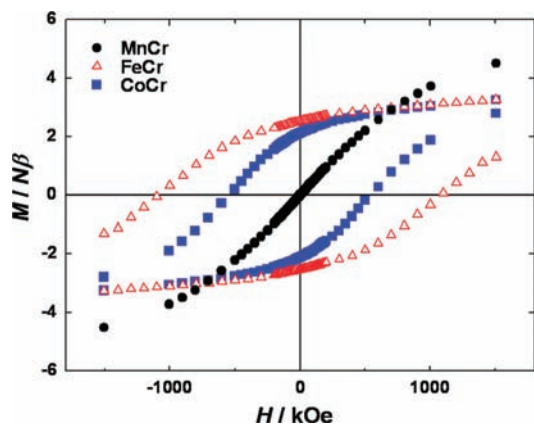


Figure 6. Hysteresis curves of the complexes measured at 2 K.

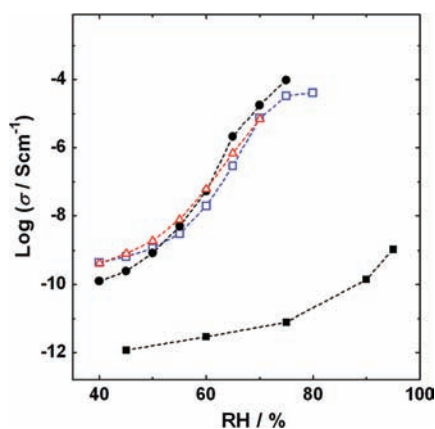


Figure 7. $\text{Log } \sigma$ (S cm^{-1}) versus RH plots of the complexes (●, MnCr; Δ, FeCr; □, CoCr) and $\{\text{N}(n\text{-C}_4\text{H}_9)_4\}[\text{MnCr}(\text{ox})_3]$ (■) at 25 °C.

the FeCr complex and the CoCr complex are 1000 and 500 Oe, respectively.

Proton Conduction. Electrical conductivities of the complexes were measured at 25 °C in the relative humidity (RH) range 40–95% by a complex-plane impedance method. Figure 7 shows the $\text{log } \sigma$ (S cm^{-1}) versus RH plots of the complexes under 40–75% RH (the complexes decomposed under >75% RH). Figure 7 also shows, as reference, the $\text{log } \sigma$ (S cm^{-1}) versus RH plots of $\{\text{N}(n\text{-C}_4\text{H}_9)_4\}[\text{MnCr}(\text{ox})_3]$ derived from the hydrophobic $\{\text{N}(n\text{-C}_4\text{H}_9)_4\}^+$ ion. The reference complex has a very low conductivity of $1.1 \times 10^{-12} \text{ S cm}^{-1}$ under 45% RH, which gradually increases to $1.1 \times 10^{-9} \text{ S cm}^{-1}$ under 95% RH. The electrical conductivities of $\{\text{NH}(\text{pro})_3\}[\text{MCr}(\text{ox})_3]$ ($M = \text{Mn, Fe, Co}$) under 40% RH are in the range 1.2×10^{-10} to $4.4 \times 10^{-10} \text{ S cm}^{-1}$, which is at least 2 orders of magnitude greater than the reference complex, and the conductivities increase with RH to reach a high conductivity of $\sim 1 \times 10^{-4} \text{ S cm}^{-1}$ around 75% RH. Evidently the high proton conduction is attributable to the 2-D hydrophilic layers formed by $\{\text{NH}(\text{pro})_3\}^+$ ions in the network structure.

To gain an insight into the proton conduction, water adsorption isotherms were measured (Figure 8). The water content per MCr unit continuously increases with RH until an abrupt increase due to complex decomposition at $\sim 70\%$ RH in the MnCr complex, $\sim 75\%$ RH in the FeCr complex, and $\sim 80\%$ RH in the CoCr complex. The isotherms in Figure 8 are drawn in the range slightly lower than the respective decomposing RH so as to allow the measurement of the water desorption process. Under $\sim 40\%$ RH, two water molecules are involved in the

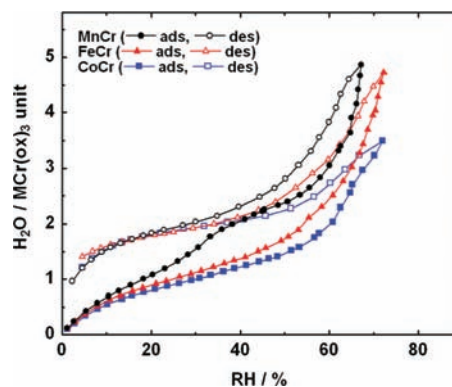


Figure 8. Water adsorption (ads) and desorption (des) isotherms of the complexes.

MnCr complex and one water molecule is involved in the FeCr and CoCr complexes in the adsorption process, while two water molecules are involved in all of the complexes in the desorption process. Obviously, the hydrogen-bonded network formed by the bimetallic layer, $\{\text{NH}(\text{pro})_3\}^+$ ions, and water molecules (two per MCr) is responsible for the proton conduction under $\sim 40\%$ RH (cf. Figure 1). In the RH region higher than 40%, the water content increases with RH to $n(\text{H}_2\text{O}) = 5$ in the MnCr and the FeCr complexes. The apparent water content in the CoCr complex is 3.5 under 73% RH, but the content comes close to 5 near 80% RH. Therefore, three water molecules (per MCr), in addition to water molecules bound to the lattice, are concerned with the high proton conduction under 75–80% RH. It is evident that the additional water molecules are much more mobile than those bound to the lattice to bring about the high proton conduction of $\sim 1 \times 10^{-4} \text{ S cm}^{-1}$. The hydrogen-bonded network formed by the bimetallic layer, $\{\text{NH}(\text{pro})_3\}^+$ ions, and water molecules is moderately effective in proton conduction, but the network facilitates the uptake of water molecules contributing to an enhancement in proton conduction under high RH. The significance of water molecules in the proton conduction has been documented.³⁴ The Grothuss mechanism³⁵ and Vehicle mechanism³⁶ have been proposed in an effort to interpret proton conduction. Which mechanism is operative in the present complexes requires further study.

Although they are sensitive to moisture, $\{\text{NH}(\text{pro})_3\}[\text{MCr}(\text{ox})_3] \cdot \text{H}_2\text{O}$ ($M = \text{Mn, Fe, Co}$) complexes are better proton conductors than the dithiooxamidato complexes,¹⁸ N,N' -bis(2-hydroxyethyl)dithiooxamidatocopper(II) ($\sigma = 1.2 \times 10^{-5} \text{ S cm}^{-1}$ under 83% RH) and N,N' -bis(3-hydroxypropyl)dithiooxamidatocopper(II) ($\sigma = 3.3 \times 10^{-9} \text{ S cm}^{-1}$ under 58% RH and $\sim 2.0 \times 10^{-6} \text{ S cm}^{-1}$ under 100% RH). The present work reveals that oxalate-bridged bimetallic complexes of hydrophilic cations are promising for developing proton-conducting materials.

It is reported that dehydration-hydration operation^{37–40} and humidity variation⁴¹ give rise to a drastic change in the bulk magnetism of some magnetic compounds, but proton-conductive

(34) Sumner, J. J.; Creager, S. E.; Ma, J. J.; DesMarteau, D. D. *J. Electrochem. Soc.* **1998**, *145*, 107.

(35) (a) Howe, A. T.; Shilton, M. G. *J. Solid State Chem.* **1980**, *24*, 149. (b) Bernard, L.; Fitch, A.; Wright, A. F.; Fender, B. E. F.; Howe, A. T. *Solid State Ionics* **1981**, *5*, 459.

(36) Kreuer, K.; Rabenau, A.; Weppner, W. *Angew. Chem., Int. Ed. Engl.* **1982**, *21*, 208.

(37) Kurmoo, M.; Kumagai, H.; Chapman, K. W.; Kepert, C. J. *Chem. Commun.* **2005**, 3012.

(38) Yoshida, Y.; Inoue, K.; Kurmoo, M. *Inorg. Chem.* **2009**, *48*, 267.

(39) Usuki, N.; Ohba, M.; Okawa, H. *Bull. Chem. Soc. Jpn.* **2002**, *75*, 1693.

properties of the magnetic compounds are not examined. To the best of our knowledge, $\{\text{NH}(\text{pro})_3\}[\text{MCr}(\text{ox})_3]$ ($\text{M} = \text{Mn}, \text{Fe}, \text{Co}$) complexes are the first complex system exhibiting the coexistence of ferromagnetism and high proton conduction.

Conclusion

The oxalate-bridged bimetallic complexes $\{\text{NH}(\text{pro})_3\}-[\text{M}^{\text{II}}\text{Cr}^{\text{III}}(\text{ox})_3]$ ($\text{M} = \text{Mn}^{\text{II}}, \text{Fe}^{\text{II}}, \text{Co}^{\text{II}}$) with the hydrophilic tri(3-hydroxypropyl)ammonium ion were prepared by the reaction of $(\text{NH}_4)_3[\text{Cr}(\text{ox})_3]$, $\text{MCl}_2 \cdot n\text{H}_2\text{O}$ and $\{\text{NH}(\text{pro})_3\}\text{Cl}$ in methanol. A crystallographic study of $\{\text{NH}(\text{pro})_3\}[\text{MnCr}(\text{ox})_3] \cdot 2\text{H}_2\text{O}$ reveals a structure based on the oxalate-bridged bimetallic layers intercalated by $\text{NH}(\text{pro})_3^+$ cations. The $\text{NH}(\text{pro})_3^+$ ions assume a tripodal configuration and interact with the bimetallic layer through hydrogen bonding. One water molecule exists in each honeycomb cavity, deviating by 1.14 Å from the Cr_3Mn_3 least-squares plane, and is statistically hydrogen bonded to three hydroxyl oxygen atoms from separate $\text{NH}(\text{pro})_3^+$ ions. The layer–cation interaction gives rise to a short interlayer separation of 7.90 Å and the unsymmetrical faces to the bimetallic layer. Cryomagnetic studies demonstrate ferromagnetic ordering, with T_C of 5.5 K for the MnCr complex, 9.5 K for the FeCr complex, and 10.0 K for the CoCr complex. It is found that the interlayer magnetic interaction is negligibly weak despite the short interlayer separation. In all of the complexes, a slow saturation in magnetization is observed, which is explained in terms of the spin canting between the M^{II} and Cr^{III} ions. They show a

proton conductivity of 1.2×10^{-10} to $4.4 \times 10^{-10} \text{ S cm}^{-1}$ under 40% RH that increases with RH to a much higher value of $\sim 1 \times 10^{-4} \text{ S cm}^{-1}$ under $\sim 75\%$ RH. Water adsorption and desorption isotherms indicate that the proton conduction under $\sim 40\%$ RH is mediated by the hydrogen-bonded network consisting of the bimetallic layer, $\text{NH}(\text{pro})_3^+$ ions, and water molecules (two per MCr). For the proton conduction under $\sim 75\%$ RH, an additional three water molecules are responsible for the high proton conduction of $\sim 1 \times 10^{-4} \text{ S cm}^{-1}$. This study reveals that the use of oxalate-bridged bimetallic complexes with hydrophilic cations appears promising for producing proton-conductive materials. This is the first example of a metal complex system exhibiting the coexistence of ferromagnetism and high proton conduction. Creation of a cooperative system of magnetism and proton conduction is our research subject in the future.

Acknowledgment. The authors thank Dr. Y. Inagaki for preliminary magnetic studies. This work was partly supported by the Grants-in-Aid for the Global COE Program, “Science for Future Molecular Systems” from the Ministry of Education, Culture, Science, Sports and Technology of Japan. A.S. and M.S. are grateful to the JSPS, Research Fellowships for Young Scientists No. 205104 and 214405.

Supporting Information Available: Powder XRD spectra of the complexes; weak-field magnetization data and AC magnetic responses of the FeCr and CoCr complexes; X-ray crystallographic data of $\{\text{NH}(\text{pro})_3\}[\text{MnCr}(\text{ox})_3] \cdot 2\text{H}_2\text{O}$ in CIF format. This material is available free of charge via the Internet at <http://pubs.acs.org>.

JA905368D

(40) (a) Yanai, Y.; Kaneko, W.; Yoneda, K.; Ohba, M.; Kitagawa, S. *J. Am. Chem. Soc.* **2007**, *129*, 3396. (b) Kaneko, W.; Ohba, M.; Kitagawa, S. *J. Am. Chem. Soc.* **2007**, *129*, 13706.

(41) Ohkoshi, S.; Arai, K.; Sato, Y.; Hashimoto, K. *Nat. Mater.* **2004**, *3*, 857.